The Astrophysical Journal, 623:1171–1179, 2005 April 20

THREE LOW-MASS PLANETS FROM THE ANGLO-AUSTRALIAN PLANET SEARCH[1]

C. G. Tinney,[2] R. Paul Butler,[3] Geoffrey W. Marcy,[4,5] Hugh R. A. Jones,[6,7] Alan J. Penny,[8,9]
Chris McCarthy,[3,5] Brad D. Carter,[10] and Debra A. Fischer[4,5]
Received 2004 September 22; accepted 2005 January 3

ABSTRACT

We report the detection of three new low-mass planets from the Anglo-Australian Planet Search. The three parent stars of these planets are chromospherically quiet main-sequence G dwarfs with metallicities ranging from roughly solar (HD 117618 and HD 208487) to metal enriched (HD 102117). The orbital periods range from 20.8 to 130 days, the minimum masses from roughly $0.5M_{\rm Sat}$ to $0.5M_{\rm Jup}$, and the eccentricities from 0.08 to 0.37, with the planet in the smallest orbit (HD 102117) having the smallest eccentricity. With semiamplitudes of 10.6–19 m s^{-1}, these planets induce Doppler amplitudes similar to those of Jupiter analogs, albeit with shorter periods. Many of the most interesting future Doppler planets will be detected at these semiamplitude levels, placing a premium on measurement precision. The detection of such amplitudes in data extending back 6 yr gives confidence in the Anglo-Australian Planet Search's ability to detect Jupiter analogs as our time baseline extends to 12 yr. We discuss the criticality of such detections for the design of the next generation of extremely large telescopes and also highlight prospects for suitable observing strategies to push to below 1 m s^{-1} precisions for bright stars in a search for sub-Neptunian planets.

Subject headings: planetary systems — stars: individual (HD 102117, HD 117618, HD 208487)

1. INTRODUCTION

The Anglo-Australian Planet Search (AAPS) began taking data in 1998 January on the nearest and brightest Sun-like stars. Results from this program (Tinney et al. 2001, 2002a, 2003; Butler et al. 2001, 2002; Jones et al. 2002, 2003; Carter et al. 2003; McCarthy et al. 2004) have demonstrated long-term velocity precisions of 3 m s^{-1} or better for suitably quiescent Sun-like stars. The AAPS, together with programs using similar techniques on the Lick 3 m and Keck 10 m telescopes (Fischer et al. 2001; Vogt et al. 2000), provides all-sky planet search coverage for inactive F, G, K, and M dwarfs out to distances of 50 pc.

AAPS is being carried out on the 3.9 m Anglo-Australian Telescope (AAT), using the University College London Echelle Spectrograph (UCLES) and an I_2 absorption cell. UCLES is operated in its 31 lines mm^{-1} mode. Prior to 2001 September it was used with an MIT/LL 2048 × 4096 15 μm pixel CCD, and since then it has been used with an EEV 2048 × 4096 13.5 μm pixel CCD. AAPS currently observes on 32 nights per year. The survey initially targeted 200 F, G, K, and M stars with $\delta < -20°$ and $V < 7.5$. Where age/activity information was available from $R'_{\rm HK}$ indices (see, e.g., Henry et al. 1996; Tinney et al. 2002b) we required target stars to have $\log R'_{\rm HK} > -4.5$, corresponding to ages greater than 3 Gyr.

In addition to the primary sample, a small subsample of 20 fainter dwarfs with *uvby* photometry suggesting metal-enrichment over solar was added in 1999 October (Tinney et al. 2003). These dwarfs have $V < 9$ and were added to examine suggestions that metal-enriched stars preferentially host planets (see, e.g., Laughlin 2000 and references therein). A further eight M dwarfs extending as faint as $V < 11$ were also included in the program. In 2002, AAPS further expanded the scope of its survey, increasing from 20 to 32 nights per year. Sixty new stars were then added to the target list, and those stars found since their initial inclusion to have $\log R'_{\rm HK}$ activity levels inconsistent with high-precision velocity measurement were culled. A signal-to-noise ratio (S/N) target $\gtrsim$200 pixel^{-1} is now standard for all stars. The AAPS target sample currently includes 234 stars.

Our observing procedure and data analysis continue to substantially follow that described in Butler et al. (1996, 2001), although over the last 12 months significant improvements have been made to the spectral extraction component of the analysis package to include features such as the automated removal of ∼97% of cosmic rays. Other improvements made to our velocity measurements include filters to ignore telluric lines in the velocity derivation and barycentric corrections that include proper motions and general relativistic effects. All data taken by the AAPS to date have now been reprocessed through this upgraded analysis system, and it is those results that we report here. Figure 1 shows long-term data for four stable stars with $B - V$ and chromospheric activity levels similar to the planet-bearing stars presented in this paper. Figure 1 of McCarthy et al. (2004) shows a different set of similarly stable AAPS stars. The velocity rms includes contributions from both measurement uncertainty and natural sources of astrophysical "jitter"—stellar oscillations, convective granulation, and the rotational modulation of surface features. In chromospherically quiet G dwarfs stellar jitter contributes 1–4 m s^{-1} to the velocity rms (Saar et al. 1998; Wright 2004). The single-shot precision of the AAPS for suitably inactive stars has been 2–3 m s^{-1} over the past 6 yr.

2. CHARACTERISTICS OF THE HOST STARS

The characteristics for each of the three host stars are summarized in Table 1—please refer to the table for references.

[1] Based on observations obtained at the Anglo-Australian Telescope, Siding Spring, Australia.
[2] Anglo-Australian Observatory, P.O. Box 296, Epping 1710; Australia. cgt@aaoepp.aao.gov.au.
[3] Carnegie Institution of Washington, Department of Terrestrial Magnetism, 5241 Broad Branch Road NW, Washington, DC 20015-1305.
[4] Department of Astronomy, University of California, Berkeley, CA 94720.
[5] Department of Physics and Astronomy, San Francisco State University, San Francisco, CA 94132.
[6] Centre for Astrophysics Research, University of Hertfordshire, Hatfield AL10 9AB, UK.
[7] Astrophysics Research Institute, Liverpool John Moores University, Twelve Quays House, Egerton Wharf, Birkenhead CH41 1LD, UK.
[8] Rutherford Appleton Laboratory, Chilton, Didcot, Oxon OX11 0QX, UK.
[9] SETI Institute, 515 North Whisman Road, Mountain View, CA 94043.
[10] Faculty of Sciences, University of Southern Queensland, Toowoomba 4350, Australia.

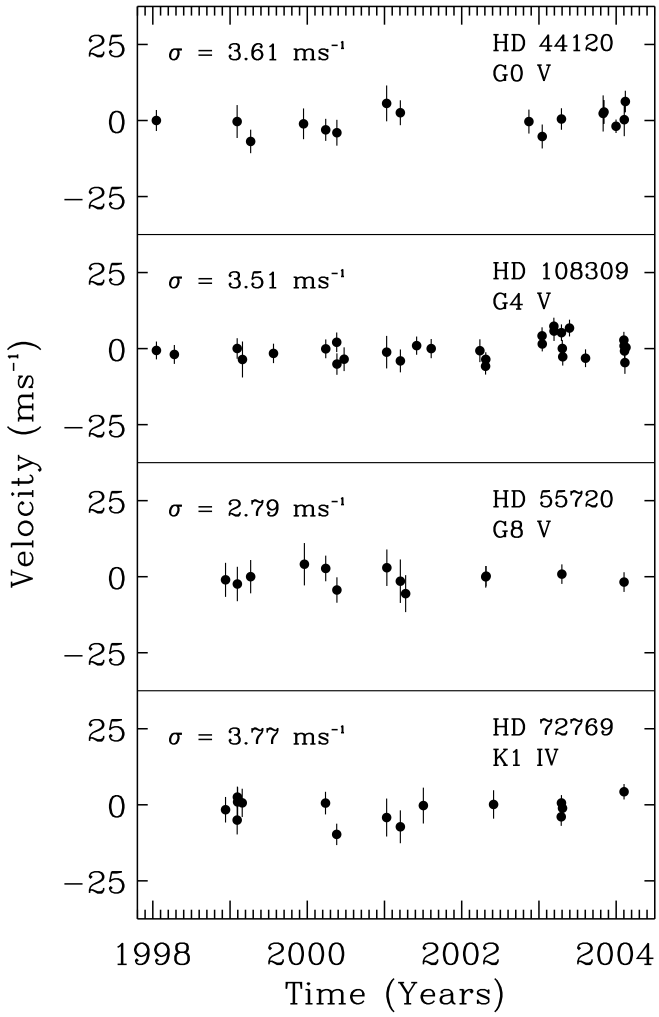

FIG. 1.—Four chromospherically quiet stars with $B - V$ and spectral types similar to the planet-bearing stars presented in this paper. The long-term single-shot precision of the AAPS is 2–3 m s^{-1} for suitable inactive stars.

HD 117618 (HIP 66047, SAO 224228).—This is a chromospherically quiet G2 V star, which was found to photometrically stable by the *Hipparcos*[11] satellite (Perryman 1997). The table compares metallicities derived from a detailed LTE spectroscopic analysis of these three stars by Fischer & Valenti (2004), the spectroscopic analysis of Bond et al. (2004), and metallicities derived from Strömgren *uvby* photometry from the General Catalogue of Photometric Data[12] (Mermilliod et al. 1997), using both the *uvby* calibration of Schuster & Nissen (1989) and a more recent recalibration by Haywood (2002). The Schuster & Nissen calibration provides systematically lower metallicities for these stars by $\approx$0.07 dex. For HD 117618 the spectroscopic and photometric metallicities are in good agreement. The $b - y$ colors of these stars also permit the estimation of effective temperatures using the calibration of Mermilliod et al. (1997) and Olsen (1984). From HD 117618's $\log R'_{\rm HK} = -4.90$, we estimate intrinsic stellar velocity jitter to be in the range 2–4 m s^{-1} (Saar et al. 1998).

Figure 2 shows evolutionary tracks at [Fe/H] = −0.05, +0.05, and +0.17 for stars of near-solar mass, interpolated from the compilation of Girardi et al. (2000). (The metallicities to which the models are interpolated correspond to the stars under consideration.) On the basis of these models and the metallicity measurements for HD 117618, its mass is estimated to be $1.05 \pm 0.05\ M_\odot$. Estimated age ranges are also indicated in Table 1.

HD 208487 (HIP 108375, SAO 213432).—This is another G2 dwarf, with a $\log R'_{\rm HK}$ measurement suggesting low chromospheric activity. *Hipparcos* finds it to be photometrically stable. Metallicity, $T_{\rm eff}$, and mass and age estimates (based on the tracks in Fig. 2) are shown in Table 1, as for HD 117618.

HD 102117 (HIP 57291, SAO 239348).—This is a G6 V dwarf, which *Hipparcos* found to be photometrically stable. Metallicity, $T_{\rm eff}$, and mass and age estimates (based on the tracks in Fig. 2) are shown in Table 1 as before. There is no published $\log R'_{\rm HK}$ measurement for HD 102117. Because the velocity amplitude observed in this star is small, a Ca HK spectrum was acquired to determine the level at which our results could be affected by activity. Figure 3 shows this spectrum for HD 102117 compared to those for several objects of similar spectral types with measured $\log R'_{\rm HK}$ values (Tinney et al. 2002b). HD 102117

[11] All *Hipparcos* data referred to in this paper were obtained from http://astro.estec.esa.nl/Hipparcos/HIPcatalogueSearch.html.

[12] Data obtained from http://obswww.unige.ch/gcpd/gcpd.html.

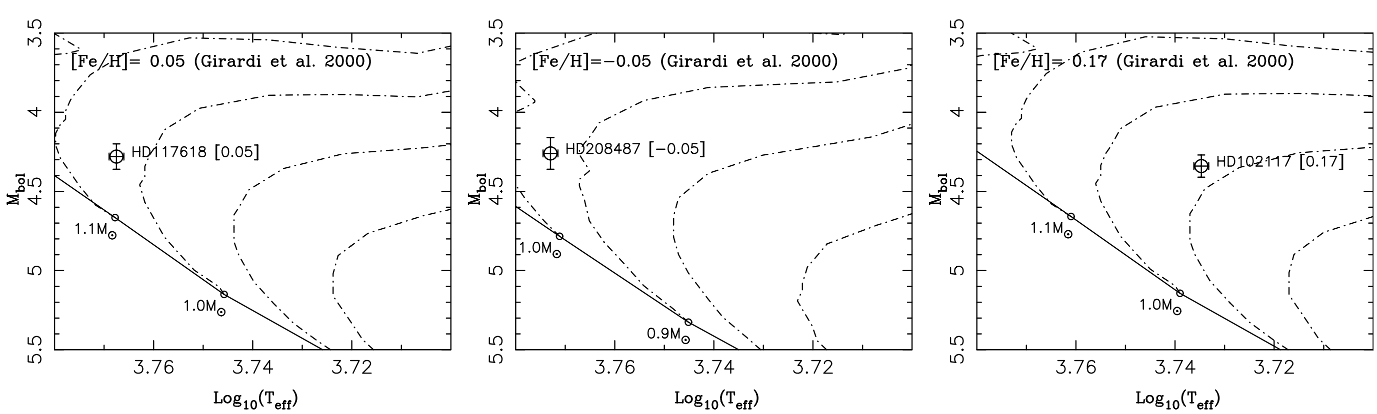

FIG. 2.—Evolutionary tracks from the compilation of Girardi et al. (2000), interpolated to the estimated metallicities for stars under discussion in this paper. The zero-age main sequence is shown as a solid line, with evolutionary models at the indicated masses shown as dot-dashed lines. The open circles and uncertainties indicate the stars, with their estimated metallicities indicated in brackets.

TABLE 1
Stellar Parameters

Parameter	HD 117618	HD 208487	HD 102117
$\log R'_{HK}$	−4.90[a]	−4.90[a]	<−5.0[b]
Hipparcos N_{obs}[c]	82	90	129
Hipparcos σ[c]	0.0012	0.0012	0.0009
Hipparcos π[d] (mas)	26.3 ± 0.9	22.7 ± 1.0	16.8 ± 0.7
M_V[c]	4.28 ± 0.08	4.26 ± 0.1	4.34 ± 0.07
M_{bol}[e]	4.08 ± 0.08	4.06 ± 0.1	4.13 ± 0.07
Spectral type	G2 V[f]	G2 V[g]	G6 V[h]
[Fe/H] (*uvby* S and N)[i]	−0.02 ± 0.16	−0.15 ± 0.16	+0.09 ± 0.16
[Fe/H] (*uvby* H)[j]	+0.04 ± 0.16	−0.06 ± 0.16	+0.16 ± 0.16
[Fe/H] (spec. B)[k]	+0.04 ± 0.08	...	+0.18 ± 0.07
[Fe/H] (spec. F and V)[l]	+0.03 ± 0.05	+0.06 ± 0.05	+0.28 ± 0.05
$T_{eff}(b-y)$[m] (K)	5855 ± 20	5929 ± 20	5429 ± 20
Mass[n] ($M_\odot$)	1.05 ± 0.05	0.95 ± 0.05	0.95 ± 0.05
Age (Gyr)[n]	4.8–6.3	6.3–10	>10

[a] Henry et al. (1996).
[b] This paper.
[c] Perryman (1997).
[d] Hauck & Mermilliod (1997) for V and Perryman (1997) for π.
[e] Lang (1992).
[f] Houck (1978).
[g] Houck (1982).
[h] Houck & Cowley (1975).
[i] Data from Hauck & Mermilliod (1997) and calibration from Schuster & Nissen (1989).
[j] Data from Hauck & Mermilliod (1997) and calibration from eqs. (2)–(4) of Haywood (2002).
[k] Bond et al. (2004).
[l] Fischer & Valenti (2004).
[m] Hauck & Mermlliod (1997) and Olsen (1984).
[n] See § 2 and Fig. 2.

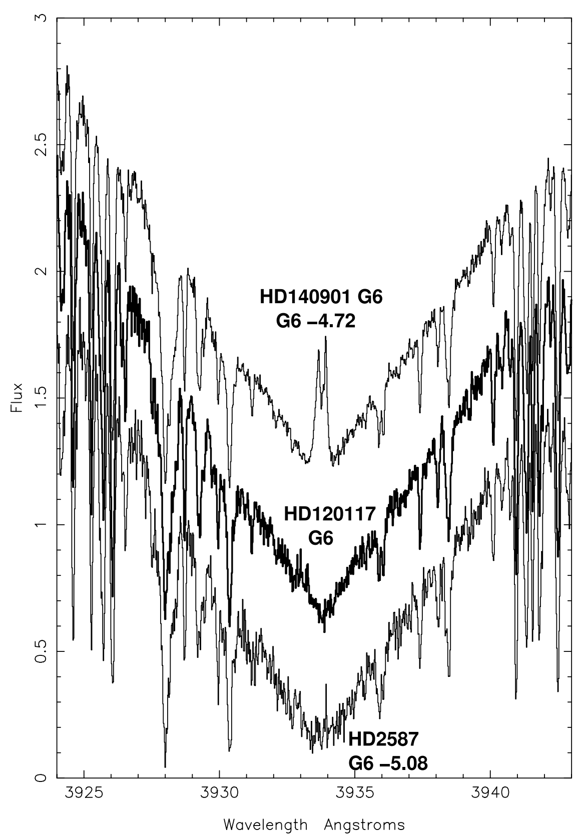

Fig. 3.—UCLES spectrum in the region of the Ca line for HD 102117 and two comparison objects of G6 spectral type with $\log R'_{HK}$ measurements from Tinney et al. (2002b)—HD 2587 with $\log R'_{HK} = -5.08$ and HD 140901 with $\log R'_{HK} = -4.72$. For each object the spectral type and measured $\log R'_{HK}$ value are shown. Based on these we assign an upper limit to the $\log R'_{HK}$ value for HD 102117 of −5.0.

shows no evidence for a line reversal—indeed it seems even less reversed than the extremely inactive ($\log R'_{HK} = -5.08$) G6 dwarf HD 2587. On the basis of this we estimate $\log R'_{HK} < -5.0$ for HD 102117, making it also very inactive, and from which we estimate its intrinsic stellar velocity jitter to be in the range 1–2 m s^{-1} or less (Saar et al. 1998).

3. RADIAL VELOCITY OBSERVATIONS AND ORBITAL SOLUTIONS

HD 117618.—Forty-seven observations of HD 117618 are shown in Figure 4 and listed in Table 2. The rms velocity for

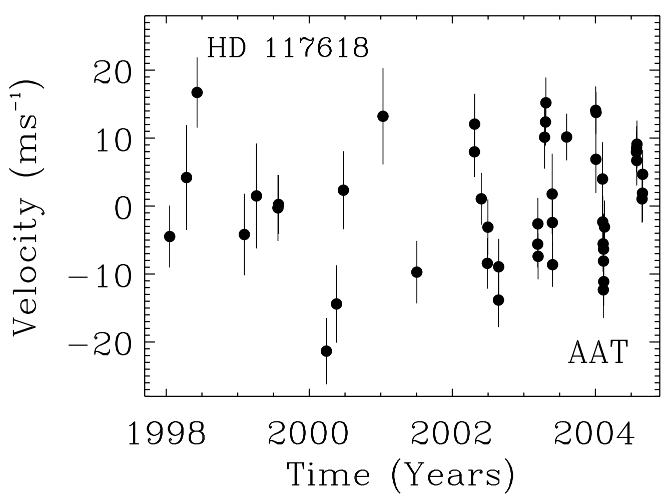

Fig. 4.—Measured velocities of HD 117618. The rms is 9.0 m s^{-1} compared to the median internal measurement uncertainty of 4.1 m s^{-1} and the expected level of stellar jitter of 2–4 m s^{-1}.

TABLE 2
VELOCITIES FOR HD 117618

JD[a] (−2,450,000)	Rest Velocity[b] (m s^{-1})	Uncertainty (m s^{-1})
831.1860	−6.3	4.6
917.1010	2.4	7.7
970.9493	14.9	5.2
1212.2061	−6.0	6.0
1274.2446	−0.3	7.7
1383.9311	−2.0	4.9
1386.8584	−1.5	4.3
1631.2594	−23.1	4.9
1682.9767	−16.2	5.7
1718.0345	0.6	5.7
1920.2631	11.4	7.1
2092.9634	−11.5	4.6
2387.0401	6.2	3.7
2388.0793	10.3	4.5
2422.0089	−0.7	3.8
2452.9768	−10.2	3.7
2455.9258	−4.9	4.1
2509.8727	−15.6	4.0
2510.8723	−10.7	4.1
2710.1776	−7.4	3.4
2710.9676	−4.4	3.8
2712.0758	−9.2	3.4
2745.1436	8.4	4.6
2750.1033	10.6	3.5
2752.0889	13.4	3.7
2784.0007	−0.0	5.9
2785.0644	−4.2	3.3
2785.9883	−10.4	3.3
2857.8802	8.4	3.4
3006.2429	12.3	3.5
3007.2413	5.1	4.9
3008.2384	12.0	3.0
3041.2336	2.2	5.4
3042.2293	−4.1	3.8
3044.1669	−7.3	4.1
3045.2784	−14.1	4.2
3046.0871	−9.9	4.5
3046.2798	−8.1	5.2
3047.2017	−12.9	3.5
3051.1948	−4.9	3.9
3213.9939	6.2	3.0
3214.8940	6.8	3.2
3215.8918	4.9	3.7
3216.9263	7.3	3.5
3242.9039	−0.7	3.5
3244.9471	0.1	4.2
3245.8814	2.9	3.6

[a] Julian dates (JD) are barycentric.
[b] Radial velocities are barycentric, but they have an arbitrary zero-point determined by the radial velocity of the template.

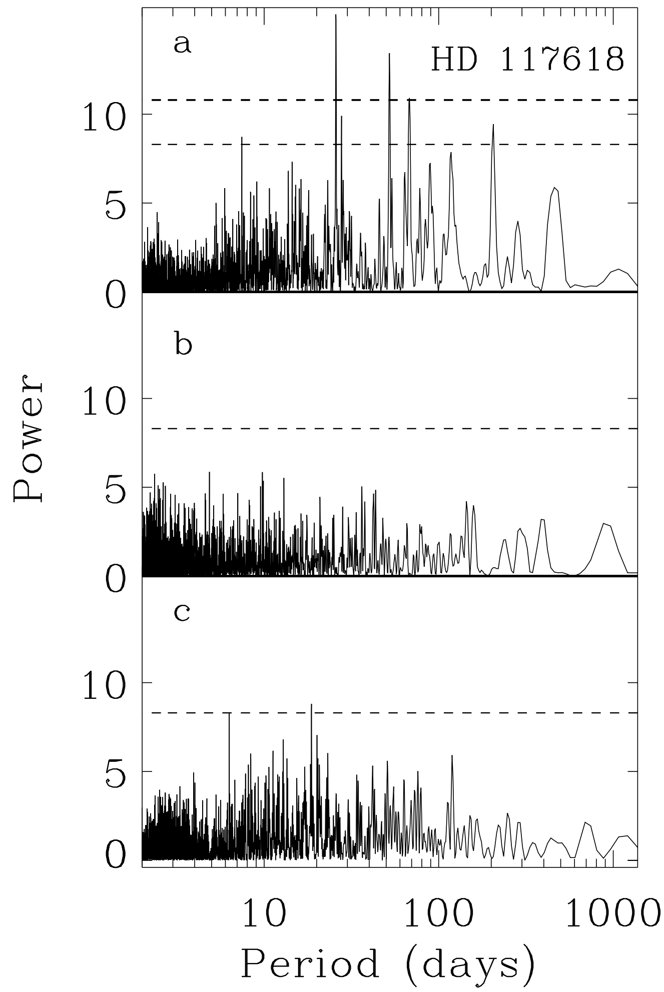

FIG. 5.—Periodograms of the 47 observations of HD 117618 obtained at the AAT between 1998 January and 2004 August. The false alarm probabilities provided are based on the assumption of normally distributed errors. (*a*) Periodogram of all velocities. The top dashed line is the 0.1% false alarm level, while the bottom dashed line is the 1% false alarm level. The two highest peaks are at the two possible periods of 25.8 and 52.2 days. (*b*) Periodogram of velocity residuals after removing the best-fit Keplerian with a period of 25.8 days. The dashed line is the 1% false alarm level. (*c*) Periodogram of velocity residuals after removing the best-fit Keplerian with a period of 52.2 days. The dashed line is the 1% false-alarm level.

HD 117618 is 9.0 m s^{-1}, while the median internal measurement uncertainty is 4.1 m s^{-1}. Activity measurements for this star (see above) suggest an intrinsic jitter in the range 2–4 m s^{-1}, strongly indicating additional velocity variability above that due to activity and measurement uncertainty alone.

A periodogram analysis (Fig. 5*a*) reveals two periodicities at well over the 0.1% false alarm rate, with the peak at 25.8 days stronger than the peak at 52.2 days. Figures 6*a* and 6*b* shows the best-fit Keplerians at these two periods. Both the rms and reduced χ^2 of these fits favor the 25.8 day period. A periodogram of the residuals after the removal of each of these Keplerians fits is shown in Figures 5*b* and 5*c*. No significant periodicities remain after removing the 25.8 day Keplerian, while the residuals to the 52.2 day Keplerian show power at the 1% level, again suggesting the 25.8 day period to be more probable. The resultant orbital parameters listed in Table 3.

HD 208487.—Thirty-one observations of HD 208487 are shown in Figure 7 and listed in Table 4. The rms of the velocities is 15.4 m s^{-1}, while the median internal uncertainty is 5.4 m s^{-1}. Periodogram analysis, shown in Figure 8, yields a dominant peak at 130 days, with a false-alarm probability of 0.4%. A more robust Monte Carlo test with full Keplerian fitting (Marcy et al. 2005) finds the same peak with a false-alarm probability of less than 0.1%. The best-fit Keplerian, shown in Figure 9, has a period of 130 days, an eccentricity of 0.29, and a semiamplitude of 19 m s^{-1}. The Keplerian orbital parameters are listed in Table 3.

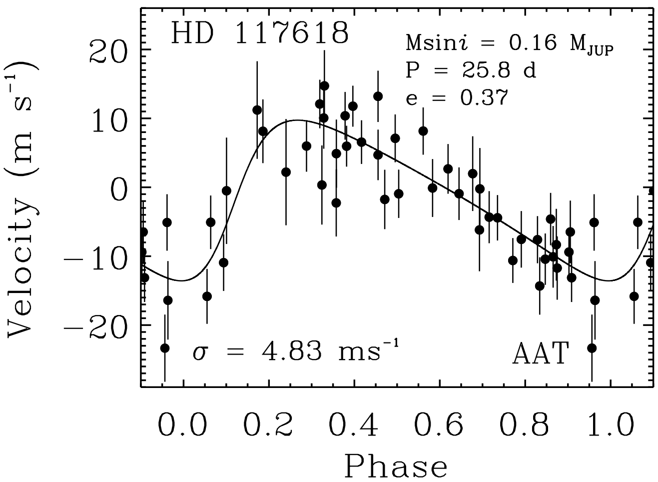

FIG. 6*a*

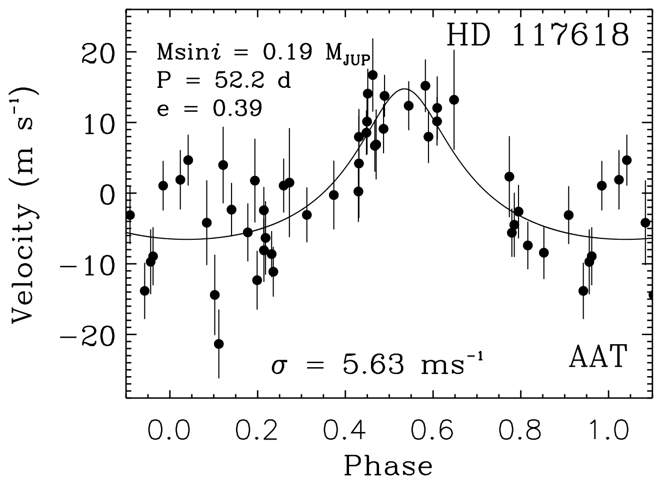

FIG. 6*b*

FIG. 6.—AAT Doppler velocities for HD 117618 phased to the best-fit Keplerian orbits at 25.8 days (*left*) and 52.2 days (*right*). The solid lines are Keplerian's with the orbital parameters shown in Table 3. The rms of the velocities about the fits are 5.6 and 4.8 m s^{-1}, respectively. Both orbital solutions are moderately eccentric. The resultant parameters for the companions are $0.19 M_{\rm Jup}$ at a semimajor axis of 0.28 AU, and $0.16 M_{\rm Jup}$ at a semimajor axis of 0.17 AU.

TABLE 3

ORBITAL PARAMETERS

Parameter	HD 117618[a]	HD 117618[b]	HD 208487	HD 102117[c]
Orbital period P (days)	25.8 ± 0.5	52.2 ± 0.5	130 ± 1	20.8 ± 0.1
Velocity amplitude K (m s^{-1})	12 ± 2	10.6 ± 2	20 ± 2	12 ± 2
Eccentricity e	0.37 ± 0.1	0.39 ± 0.1	0.32 ± 0.10	0.08 ± 0.05
ω (deg)	260 ± 40	359 ± 40	126 ± 40	300 ± 40
Periastron time (JD −2,450,000)	836.4 ± 2	870.3 ± 2	1002.8 ± 10	944.2 ± 1
$M \sin i$ ($M_{\rm Jup}$)	0.16 ± 0.03	0.19 ± 0.04	0.45 ± 0.05	0.18 ± 0.03
a (AU)	0.17 ± 0.01	0.28 ± 0.02	0.49 ± 0.04	0.15 ± 0.01
rms about fit (m s^{-1})	4.8	5.1	7.2	3.3
Reduced χ^2	1.10	1.29	1.27	0.89

[a] Orbital parameters for the more probable period of 25.8 days.
[b] Orbital parameters for possible period of 52.2 days.
[c] Additional slope of -1.3 ± 1.0 m s^{-1} yr^{-1} included in fit.

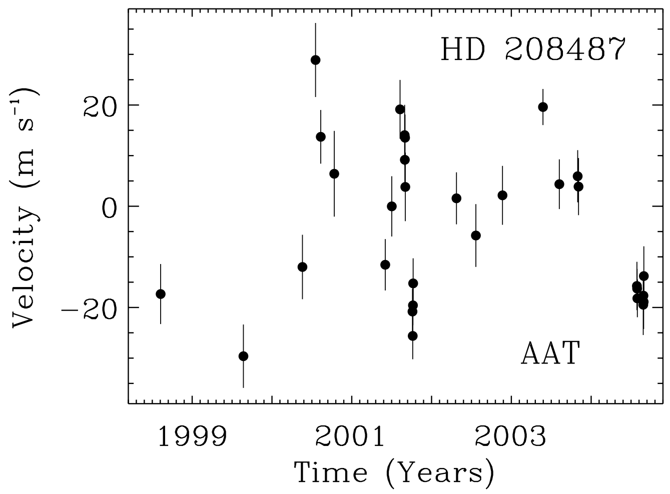

FIG. 7.—Measured velocities of HD 208487. The rms is 15.3 m s^{-1} compared to the median internal measurement uncertainty of 5.1 m s^{-1} and the expected level of stellar jitter of 2–4 m s^{-1}.

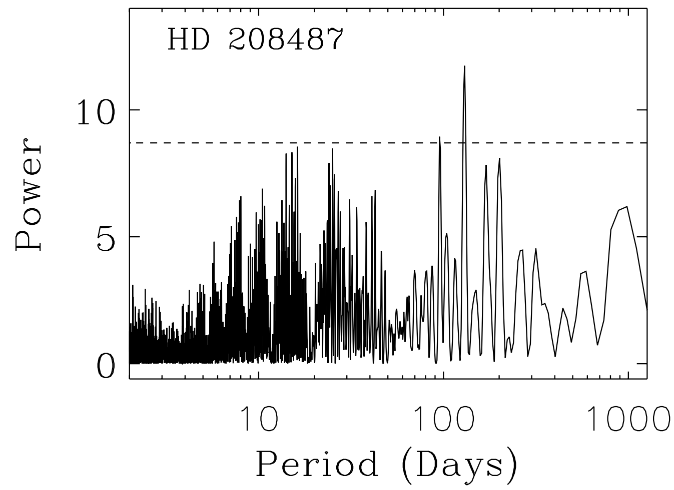

FIG. 8.—Periodograms of the 31 observations of HD 208487 obtained at the AAT between 1998 August and 2004 August. The dashed line is the 0.1% false-alarm level.

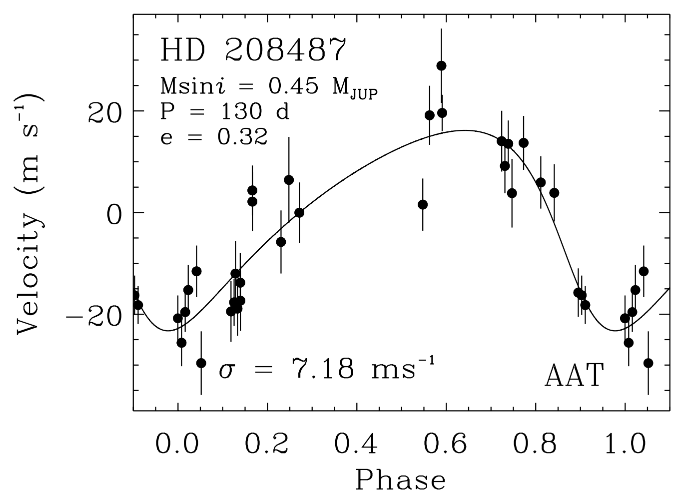

FIG. 9.—AAT Doppler velocities of HD 208487 from 1998 August to 2004 August phased to the period of the best-fit Keplerian orbit. The orbit is eccentric ($e = 0.32$), with amplitude 20 m s^{-1}, and the period is 130 days, resulting in a minimum mass ($M \sin i$) companion of $0.45 M_{\rm Jup} \pm 0.05 M_{\rm Jup}$ and semimajor axis of 0.49 ± 0.04 AU. The rms of the velocities about the fit is 7.2 m s^{-1}.

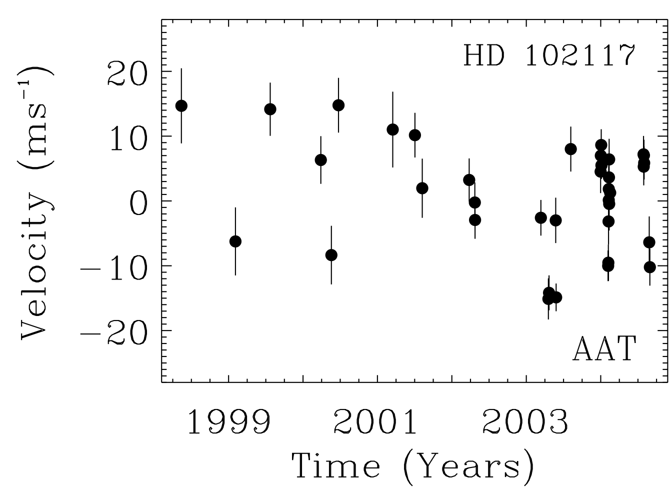

FIG. 10.—Measured velocities of HD 102117. The rms is 8.26 m s^{-1} compared to the median internal measurement uncertainty of 3.2 m s^{-1} and the expected level of stellar jitter of 2–4 m s^{-1}.

TABLE 4
VELOCITIES FOR HD 208487

JD[a] (−2,450,000)	Rest Velocity[b] (m s^{-1})	Uncertainty (m s^{-1})
1034.1784	−10.0	5.9
1413.0959	−22.3	6.3
1683.2859	−4.7	6.4
1743.2034	36.2	7.3
1767.1218	21.1	5.3
1828.9367	13.8	8.5
2062.2845	−4.2	5.1
2092.1860	7.3	6.0
2130.0900	26.5	5.8
2151.0609	21.4	6.0
2151.9939	16.5	5.4
2152.9746	20.9	4.6
2154.0554	11.2	6.8
2186.9371	−13.5	4.5
2188.0133	−18.3	4.6
2189.0752	−12.2	3.9
2189.9596	−7.9	5.0
2388.3075	8.9	5.1
2477.1633	1.6	6.2
2598.9457	9.5	5.8
2784.2671	26.9	3.6
2859.1422	11.7	4.9
2943.0690	13.3	5.2
1946.9954	11.2	5.6
3214.1904	−8.4	4.8
3215.1841	−8.9	3.9
3216.2225	−10.9	3.7
3243.2487	−12.1	6.0
3244.1456	−10.3	4.6
3245.1404	−11.5	5.4
3245.9354	−6.5	5.9

[a] Julian dates (JD) are barycentric.
[b] Radial velocities are barycentric, but they have an arbitrary zero-point determined by the radial velocity of the template.

TABLE 5
VELOCITIES FOR HD 102117

JD[a] (−2,450,000)	Rest Velocity[b] (m s^{-1})	Uncertainty (m s^{-1})
946.9573	14.0	5.8
1212.2223	−6.9	5.3
1382.8953	13.5	4.1
1631.2201	5.7	3.7
1682.9513	−9.0	4.5
1717.9992	14.1	4.2
1984.0868	10.4	5.8
2092.9359	9.5	3.4
2128.9192	1.3	4.6
2359.1402	2.6	3.3
2386.9804	−0.9	3.1
2388.0219	−3.6	2.9
2711.0584	−3.2	2.8
2747.9962	−15.8	3.2
2751.0643	−14.8	2.7
2783.9325	−3.6	3.5
2785.9589	−15.5	2.1
2857.8613	7.4	3.5
3004.2480	3.9	3.3
3005.2438	6.3	2.4
3007.2001	8.0	2.4
3008.1976	4.9	2.1
3041.1643	−10.7	2.4
3042.1163	−10.2	2.8
3043.0897	−3.8	3.6
3044.1573	−0.5	2.6
3044.2802	1.2	3.6
3045.2683	3.0	2.7
3046.0968	5.8	3.2
3046.2682	−1.1	4.1
3051.1781	0.6	2.6
3214.8548	6.5	2.8
3215.8494	4.7	2.9
3216.8419	6.4	2.4
3217.8407	5.2	2.5
3242.8835	−7.0	4.0
3245.8605	−10.9	2.9

[a] Julian dates (JD) are barycentric.
[b] Radial velocities are barycentric, but they have an arbitrary zero-point determined by the radial velocity of the template.

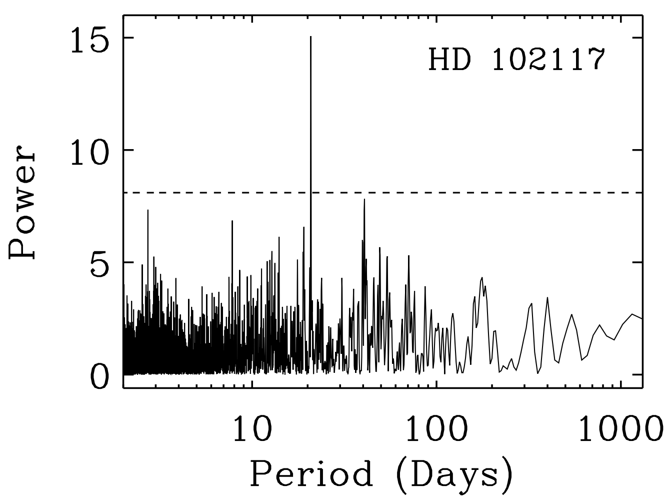

FIG. 11.—Periodogram of HD 102117 velocities. The dotted lines shows the 0.1% false-alarm level. The single dominant period is at 20.8 days.

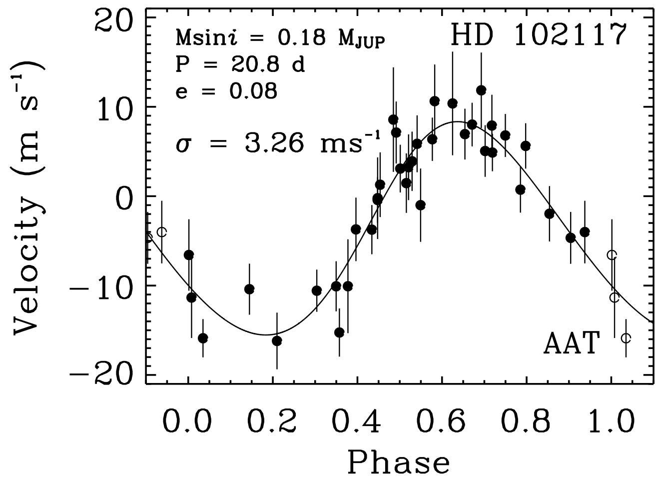

FIG. 12.—AAT Doppler velocities for HD 102117 from 1998 May to 2004 August, phased at the best-fit Keplerian period of 20.8 days. The orbit is nearly circular ($e = 0.08$), and the amplitude is 12 m s^{-1}. The resultant minimum mass ($M \sin i$) of the companion is $0.18 M_{\rm Jup} \pm 0.03 M_{\rm Jup}$ with a semimajor axis of 0.15 ± 0.01 AU. The rms of the velocities about the fit is 3.3 m s^{-1}.

The rms to the fit is 7.23 m s^{-1}, and the reduced χ^2 to the fit is 1.29.

HD 102117.—Thirty-seven observations of HD 102117 are shown in Figure 10 and listed in Table 5. Figure 11 shows the periodogram of the resulting velocities. The single dominant period is 20.8 days. The best-fit Keplerian orbit, shown in Figure 12, has period of 20.8 days, an eccentricity of 0.08, a semiamplitude of 12 m s^{-1}, and a minimum ($M \sin i$) mass of $0.18 M_{\rm Jup}$.

4. DISCUSSION

All three of these exoplanets have been detected in systems with velocity amplitudes of less than 20 m s^{-1}. The ability of the AAPS to detect such low-amplitude planets—even when the parent stars are as faint as $V = 7.5$—highlights the outstanding control of systematic errors that our new and improved reduction algorithms deliver.

Extrasolar planets with periods of less than 5 days typically have circular orbits owing to tidal circularization. The upper bound on eccentricity increases with semimajor axis out to 0.5 AU, where it tops out at $e \sim 0.7$ (Marcy et al. 2003). Both low-mass and high-mass planets follow this pattern (Jones et al. 2004), as do the three planets announced here.

4.1. *The Future of Doppler Searches*

Of the ~140 known extrasolar planets,[13] the median Doppler semiamplitude is 53 m s^{-1}. These planets were discovered first precisely because they have the largest Doppler semiamplitudes. Even within this self-selected group of the most massive planets, the planet mass function rises steeply down to the detection limit near $1 M_{\rm Jup}$ (Marcy et al. 2003; Jones et al. 2004). A critical question is whether the mass function continues to rise down to the Saturn- and Neptune-mass range.

Given the intrinsic difficulty of finding small-amplitude planets, it is not surprising that only nine have entered the refereed literature to date—most within the last 2 yr.[14] Measurement

[13] See http://www.ciw.edu/boss/IAU/div3/wgesp/planets.shtml.
[14] HD 49674 (Butler et al. 2003); 55 Cnc c (Marcy et al. 2002a); HD 3651 (Fischer et al. 2003); HD 16141 (Marcy et al.2000); HD 4208 (Vogt et al. 2002); HD 114729 (Butler et al. 2003); 47 UMa c (Fischer et al. 2002); HD 190360 (Naef et al. 2003); HR 1084 (Hatzes et al. 2000); 55 Cnc e (McArthur et al. 2004); Gl 436 (Butler et al. 2004b); and HD160691 d (Santos et al. 2004).

TABLE 6
ASTEROSEISMOLOGY FOR SOLAR-TYPE STARS

Star	Spectral Type	$\hat{V}$ (m s^{-1})	*p-p* (m s^{-1})	rms (m s^{-1})	$P_{\rm obs}$ (minutes)
Sun	G2 V	0.23[a]	...	...	5[a]
α Cen A	G2 V	0.35[a]	2[b]	...	6.7[b]
α Cen B	K1 V	0.14[c]	1.5[d]	0.5[d]	4[d]
β Hyi	G2 IV	0.51[a]	5[d]	1.7/3.3[e]	16.6[e]
HD 20794	G8 V	0.39[f]	2.5[d]	0.8[d]	5[d]
HD 160691	G5 IV	0.39[f]	5[d]	1.7[d]	9[d]

[a] Houdek & Gough (2002).
[b] Butler et al. (2004a).
[c] Carrier & Bourban (2003).
[d] Mayor et al. (2003).
[e] Bedding et al. (2001).
[f] Bouchy (2004).

precision is the single most important tool in the search for these elusive quarry. Demonstrations, via the publication of stable star results, of 2–3 m s^{-1} long-term precisions, have been shown by the Doppler programs at Keck (Vogt et al. 2000; Butler et al. 2004b), Lick (Fischer et al. 2001), VLT2 (Kürster et al. 2003), and at the AAT (McCarthy et al. 2004; Butler et al. 2001; this paper).

Almost all of the 2000 nearest and brightest Sun-like stars out to 50 pc, which are suitable for precision Doppler study, have now been under survey for more than a year. Many have been under study for more than 3 yr, and some for as long as 15 yr. The few remaining large-amplitude planets in this sample of stars will emerge within the next few years—thereafter most Doppler planets will have semiamplitudes of less than 20 m s^{-1}. These systems are also the most compelling since they include both solar system analogs with periods of 10–30 yr and semiamplitudes of 3–10 m s^{-1} and potentially rocky 10 $M_\oplus$ "super-Earths" in small orbits.

4.2. *Asteroseismology as Noise*

The primary scientific goal of the AAPS program is the detection of such small-amplitude systems. What are the fundamental limits (other than those set by photon counting) to the precision achievable by Doppler velocity programs? One source of noise that has come into focus recently is asteroseismology. Results in this field (e.g., Butler et al. 2004a; Kjeldsen et al. 2003; Mayor et al. 2003) have highlighted the prospect that *p*-mode seismological oscillations in stars may indeed be a dominant source of the noise currently seen in high-precision Doppler programs for bright stars. These oscillations have now been detected in several stars (see, e.g., Bedding & Kjeldsen 2003; Bouchy & Carrier 2003)—Table 6 summarizes some recent results in this fast moving field. It highlights the fact that while the power levels observed in the peak modes of these stars' power spectra ($\hat{V}$) are small, the stars invariably show significant peak-to-peak velocity excursions as the various incoherent modes interact. These can induce *significant* (i.e., 1–2 m s^{-1}) Doppler scatter into observations with exposure times less than the fundamental period. However, the available asteroseismology also shows us that most of the signal in these *p*-mode power spectra falls at frequencies within $\pm$50% of the peak frequency. This strongly suggests that an observing strategy that targets several integer multiples of the time corresponding to that peak frequency will integrate over the major oscillations, delivering 1–2 m s^{-1} less jitter. For the AAPS, observations of bright stars ($V < 6$), in particular, can collect sufficient photons to deliver photon-limited precisions of $\lesssim$1 m s^{-1} (i.e., S/N $>$ 500) in exposures of less than a few minutes. These short observations will clearly have been strongly affected by asteroseismological noise. However, the flip side of this situation is that improved observing strategies will open a new regime of $\lesssim$1 m s^{-1} precision, allowing the detection of Neptune and sub-Neptune mass planets in short orbits around these bright stars.

4.3. *Solar System Analogs and Extremely Large Telescopes*

Detecting a meaningful number (i.e., 10 or more) of habitable terrestrial planets is one of the key science drivers for the next generation of extremely large telescopes (ELTs) and space-based planet finders. These major new facilities will require the expenditure of billions of dollars and/or euros. Assuming that the technical problems of light suppression can be solved to the required levels (e.g., $>10^{-10}$ suppression of light from the parent star over 10–500 mas), the diameter that such a telescope has to have scales directly with how common such planets are. If they are found around 10% of Sun-like stars, then an ELT needs to be able to resolve terrestrial planets around only a hundred nearby stars. If they are found around 1% of Sun-like stars, then our ELTs need to target a thousand nearby stars. Unfortunately, the number of nearby stars available to search is limited—100 nearby stars will necessitate targeting stars out to $\sim$10–20 pc, which can be comfortably surveyed by a telescope of diameter $D = 30$ m ($4\lambda/D \approx 30$ mas).[15] But surveying a thousand stars will force an ELT to targets at 100 pc, which itself drives the telescope to a 100 m diameter, with a consequent huge increase in both cost and complexity.

Clearly before engaging in such massive expenditures, we need to know, "How common are terrestrial planets?"—and the best answer we can get to that question will come from knowing, "How common are solar system analogs?" Radial velocity surveys operating at the precision of the AAPS, therefore, have a clear and compelling role in addressing these critical design- and cost-driving issues. With 6 yr of southern hemisphere data for almost 200 stars already under its belt, the AAPS is well placed to be a major contributor in this key scientific area in the next 5 yr.

[15] It is extremely unlikely that even the most advanced coronography will be able to make significant headway at angular separations of less than $4\lambda/D$ (see, e.g., Sivaramakrishnan et al. 2001).

The Anglo-Australian Planet Search team would like to gratefully acknowledge the support of Brian Boyle, past Director of the AAO, the contributions and assistance of Stuart Ryder, and the superb technical support that has been received throughout the program from AAT staff—in particular R. Patterson, D. Stafford, F. Freeman, S. Lee, J. Pogson, G. Kitley, and J. Stevenson. We further acknowledge support by the partners of the Anglo-Australian Telescope Agreement (C. G. T., H. R. A. J., and A. J. P.); NASA grant NAG5-8299 and NSF grant AST 95-20443 (G. W. M.); NSF grant AST 99-88087 (R. P. B.); and Sun Microsystems. NSO/Kitt Peak FTS data used here were produced by NSF/NOAO. This research has made use of the SIMBAD database, operated at CDS, Strasbourg, France, and the NASA's Astrophysics Data System.

REFERENCES

Bedding, T. R., & Kjeldsen, H. 2003, Publ. Astron. Soc. Australia, 20, 203
Bedding, T. R., et al. 2001, ApJ, 549, L105
Bond, J., et al. 2004, MNRAS, submitted
Bouchy, F. 2004, Proc. Dome C Astronomy/Astrophysics Meeting (Toulouse: CESR), http://www. cesr. fr/~moly/domec/presenta.html
Bouchy, F., & Carrier, F. 2003, Ap&SS, 284, 21
Butler, R. P. Marcy, G., Vogt, S., Fischer, D., Henry, G., Laughlin, G., & Wright, J. T. 2003, ApJ, 582, 455
Butler, R. P., Marcy, G. W., Williams, E., McCarthy, C., & Dosanjh, P. 1996, PASP, 108, 500
Butler, R. P., Tinney, C. G., Marcy, G. W., Jones, H. R. A., Penny, A. J., & Apps, K. 2001, ApJ, 555, 410
Butler, R. P., et al. 2002, ApJ, 578, 565
———. 2004a, ApJ, 600, L75
———. 2004b, ApJ, 617, 580
Carrier, F., & Bourban, G. 2003, A&A, 406, L23
Carter, B. D., Butler, R. P., Tinney, C. G., Jones, H. R. A., Marcy, G. W., McCarthy, C., Fischer, D. A., & Penny, A. J. 2003, ApJ, 593, L43
Fischer, D. A., Butler, R. P., Marcy, G. W., Vogt, S. S., & Henry, G. W. 2003, ApJ, 590, 1081
Fischer, D. A., Marcy, G. W., Butler, R. P., Laughlin, G., & Vogt, S. S. 2002, ApJ, 564, 1028
Fischer, D. A., Marcy, G. W., Butler, R. P., Vogt, S. S., Frink, S., & Apps, K. 2001, ApJ, 551, 1107
Fischer, D. A., & Valenti, J. A 2004, in IAU Symp. 219, Stars as Suns: Activity, Evolution, and Planets, ed. A. K. Dupree & A. O. Benz (San Francisco: ASP), 237
Girardi, L., Bressan, A., Bertelli, G., & Chiosi, C. 2000, A&AS, 141, 371
Hatzes, A. P., et al. 2000, ApJ, 544, L145
Haywood, M. 2002, MNRAS, 337, 151
Henry, T. J., Soderblom, D. R., Donahue, R. A., & Baliunas, S. L. 1996, AJ, 111, 439
Houck, N. 1978, Houck, N. 1978, Michigan Catalog of Two Dimensional Spectral Types for the HD Stars, Vol. 2, Michigan Spectral Survey (Ann Arbor: Univ. Michigan)
———. 1982, Michigan Catalog of Two Dimensional Spectral Types for the HD Stars, Vol. 3, Michigan Spectral Survey (Ann Arbor: Univ. Michigan)
Houck, N., & Cowley, A. P. 1975, Michigan Catalog of Two Dimensional Spectral Types for the HD Stars, Vol. 1, Michigan Spectral Survey (Ann Arbor: Univ. Michigan)
Houdek, G., & Gough, D. O. 2002, MNRAS, 336, L65
Jones, H. R. A., Butler, R. P., Marcy, G. W., Tinney, C. G., Penny, A. J., McCarthy, C., Carter, B. D., & Pourbaix, D. 2003, MNRAS, 341, 948
Jones, H. R. A., Butler, R. P., Tinney, C. G., Marcy, G. W., Penny, A. J., McCarthy, C., & Carter, B. D. 2002, MNRAS, 333, 871
Jones, H. R. A., Jenkins, J. S., & Butler, R. 2004, MNRAS, submitted
Kjeldsen, H., et al. 2003, AJ, 126, 1483
Kürster, M., et al. 2003, A&A, 403, 1077
Lang, K. R. 1992, Astrophysical Data: Planets and Stars (Berlin: Springer)
Laughlin, G. 2000, ApJ, 545, 1064
Marcy, G. W., Butler, R. P., Fischer, D. A., Laughlin, G., Vogt, S. S., Henry, G. W., & Pourbaix, D. 2002, ApJ, 581, 1375
Marcy, G. W., Butler, R. P., Fischer, D. A. & Vogt, S. S. 2003, in ASP Conf. Ser. 294, Scientific Frontiers in Research on Extrasolar Planets, ed. D. Deming & S. Seager (San Francisco: ASP), 1
Marcy, G. W., Butler, R. P., & Vogt, S. S. 2000, ApJ, 536, L43
Marcy, G. W., Butler, R. P., Vogt, S. S., Fischer, D. A., Henry, G. W., Laughlin, G., Wright, J. T., & Johnson, J. 2005, ApJ, 619, 570
Mayor, M., et al. 2003, Messenger, 114, 20
McArthur, B. E., et al. 2004, ApJ, 614, L81
McCarthy, C., et al. 2004, ApJ, 617, 575
Mermilliod, J. C., Mermilliod, M., & Hauck, B. 1997, A&AS, 124, 349
Naef, D., et al. 2003, A&A, 410, 1051
Olsen, E. H. 1984, A&AS, 57, 443
Perryman, M. A. C., ed. 1997, The *Hipparcos* and Tycho Catalogue (ESA SP-1200; Noordwijk: ESA)
Saar, S. H., Marcy, G. W., & Butler, R. P. 1998, ApJ, 498, L153
Santos N., et al. 2004, A&A, 426, L19
Schuster, W. J., & Nissen, P. E. 1989, A&A, 221, 65
Sivaramakrishnan, A., Koresko, C. D., Makidon, R. B., Berkefeld, T., & Kuchner, M. J. 2001, ApJ, 552, 397
Tinney, C. G., Butler, R. P., Marcy, G. W., Jones, H. R. A., Penny, A. J., McCarthy, C., & Carter, B. D. 2002a, ApJ, 571, 528
Tinney, C. G., Butler, R. P., Marcy, G. W., Jones, H. R. A., Penny, A. J., McCarthy, C., Carter, B. D., & Bond, J. 2003, ApJ, 587, 423
Tinney, C. G., Butler, R. P., Marcy, G. W., Jones, H. R. A., Penny, A. J., Vogt, S. S., Apps, K., & Henry, G. W. 2001, ApJ, 551, 507
Tinney, C. G., McCarthy, C., Jones, H. R. A., Butler, R. P., Carter, B. D., Marcy, G. W., & Penny, A. J. 2002b, MNRAS, 332, 759
Vogt, S. S., Butler, R. P., Marcy, G. W., Fischer, D. A., Pourbaix, D., Apps, K., & Laughlin, G. 2002, ApJ, 568, 352
Vogt, S. S., Marcy, G. W., Butler, R. P., & Apps, K. 2000, ApJ, 536, 902
Wright, J. T., Marcy, G. W., Butler, R. P., & Vogt, S. S. 2004, ApJS, 152, 261